Partial Wetting of Cylindrical Catalytic Carriers in Trickle-Bed Reactors

D. C. Tsamatsoulis and N. G. Papayannakos
Dept. of Chemical Engineering, Lab. of Chemical Process Engineering,
National Technical University of Athens, Athens, Greece

The use of a modified Thiele modulus, as a correlating parameter for partially wetted catalyst pellets, is compared with the exact solution of the diffusion and reaction problem. The study of a variety of partially wetted cylindrical catalyst pellets for first- and second-order kinetics indicates that the manner in which particles are externally wetted does not significantly influence the value of the effectiveness factor. External and internal partial wetting of industrial-size porous extrudates is determined in a bench-scale hydrotreater at real hydroprocessing conditions by simulating the system response to a step change of feed using the sulfur compounds of a petroleum fraction as tracer molecules. To solve the corresponding mass balances in the interparticle and intraparticle domain, two different numerical methods are compared.

Introduction

Observed reaction rates in trickle-bed reactors are affected by a number of factors, such as intrinsic kinetics, intraparticle mass-transfer resistances, nonidealities of liquid flow, and catalyst wetting. Intraparticle diffusion can be expressed by the effective diffusion coefficient, D_e. The liquid flow can be simulated by a model that takes backmixing phenomena into account (Sicardi et al., 1980; van Gelder and Westerterp, 1990; Tsamatsoulis, 1993). On the other hand, partial wetting of catalyst particles affects global reaction rates and catalyst effectiveness.

The role of partial wetting has been discussed by many investigators (Mears, 1974; Satterfield, 1975; Parascos and Frayer, 1975; Duducovic and Mills, 1978; Schwartz et al., 1976; Colombo et al., 1976; Giannetto et al., 1978; Morita and Smith, 1978; Sicardi et al., 1980; Herskowitz, 1981; Yentecakis and Vayenas, 1987). Partial wetting can increase or decrease the global reaction rate, which depends on the nature of the limiting reactants. When the reactants are present in the liquid phase, as they are in hydroprocessing of petroleum fractions, catalyst effectiveness increases with increased wetting. Mears (1974) proposed a correlation according to which the observed rates should be proportional to the fraction of the wetted external surface of the catalyst particles. This correlation was proved to be valid only for fast reactions occurring in the external regions of the particles. In most cases the influence of liquid contacting on catalyst performance is more complicated because the boundary conditions around the particle are not uniform and they may vary with time. Therefore, conventional expressions for the effectiveness factor cannot be applied *a priori*.

According to Colombo et al. (1976) two types of particle wetting can be considered:

1. Internal wetting, as a measure of the internal catalyst surface that is available for the reaction.
2. External effective wetting, defined as the fraction of the external surface of the catalyst particles effectively contacted by the flowing liquid. The degree of effective wetting is not generally the same as the degree of total external wetting because the semistagnant liquid around the contact points of the particles may make a minor contribution to the mass exchange rate between the wetted part and the inner part of the particles.

Approximate values of the effectiveness factor, n_{eff}, for catalysts used in trickle bed hydrotreaters can be obtained from a modified Thiele modulus $\phi_{pw} = \phi/F_w$, where ϕ denotes the Thiele modulus for complete catalyst wetting and F_w the external effective wetting according to Colombo et al. (1976) and Duducovic (1977). This approach allows for the longer actual mean path of the diffusing molecules in a partially wetted porous particle. If the effect of the partial wetting is not taken into account, the values of effective diffu-

Correspondence concerning this article should be addressed to N. G. Papayannakos.

sion coefficients and catalyst tortuosity will depend on the degree of wetting and could not be used in simulation and scale-up.

Previous investigators have described the overall effectiveness factor as a function of partial wetting for catalyst particles in the form of slabs, cylinders, and spheres (Ramanchandran and Smith, 1979; Tan and Smith, 1980; Mills and Duducovic, 1980; Herskovitz, 1981) for single and first-order reactions, and they have derived analytical solutions. Yentekakis and Vayenas (1987) analyzed the problem of the reaction between a volatile component and one or two nonvolatile components in partially wetted spheres for different locations of the wetted zones and first-order kinetics. Using two nonvolatile reactants, the evaluated order of the global reaction rate is higher than one. Goto et al. (1981) compared the values of the effectiveness factor given by approximate solutions with the ones obtained from the numerical solution of the relevant partial differential equation for one-half and second-order reactions occurring in catalytic spheres. The correlation between partial wetting and operating parameters has been studied experimentally (Colombo et al., 1976; Morita and Smith, 1978; Mills and Dudukovic, 1981). Colombo et al. (1976) attributed external effective wetting to an effective diffusion coefficient determined on the basis of a model that assumes total external catalyst wetting.

Internal particle wetting is taken into account in most of the models presented in the literature, but there are few available experimental values. Due to capillary forces, and irrespective of the degree of the external wetting, the catalyst pores should be filled with the liquid if the pores are interconnected, evenly distributed over the particle volume, and can be penetrated by the diffusing molecules. In complex mixtures, only the small molecules can diffuse and fill all the pores, but the large ones may not be able to penetrate the small pores. Then, for the reactions involving the large molecules, the internal wetting is not complete. Gianetto et al. (1978) report experimental values of internal wetting in the range of 1–0.8, and Schwartz et al. (1976) report average values of 0.78 and 0.66 determined with different measuring methods of the holdups. Schiesser and Lapidus (1961) measured a fractional pore filling equal to 0.8 when the liquid flow rate was varied by a factor of 2.5.

This article has two main objectives: to compare the analytical solution, using a modified Thiele modulus for partial wetting, with the numerical solution for cylindrical catalyst particles and for first- and second-order kinetics; and to study the contacting effectiveness of porous extrudates of industrial size in real hydroprocessing conditions in a bench-scale hydrotreater. This latter is attempted by simulating the system response to a step change of feed using as a tracer the sulfur compounds of a real feed.

Experimental Studies

Two heavy vacuum gas oils (HVGO) with similar properties at reaction conditions were used as feeds. The sulfur compounds contained in one served as tracer molecules. The other did not contain sulfur in measurable concentration. A feed swing method was employed and the response of the system was followed and analyzed. The feed gas was hydrogen of industrial purity and the flow rate was kept at 17×10^{-6} Nm^3/s throughout the experimentation. A detailed description of the experimental procedure and apparatus is given elsewhere (Tsamatsoulis and Papayannakos, 1994). Nondiluted beds of porous alumina and diluted ones with nonporous silicate powder were prepared for the experiments, and their characteristics are given in Table 1. Each experimental point was repeated 3 to 5 times, and the variance of the curves obtained was examined.

Table 1. Characteristics of the Beds

Bed 1	
Porous particles	Alumina extrudates
Mean diameter	1.4×10^{-3} m
Extrudates' true density	3.32×10^{3} kg/m^3
Extrudates' porosity	0.59
Bed porosity	0.44
Bed length	0.46 m
Bed 2	
Porous particles	Alumina extrudates
Mean dia. of extrudates	1.4×10^{-3} m
Nonporous particles	Silicate powder
Mean dia. of powder	0.35×10^{-3} m
Extrudates' true density	3.32×10^{3} kg/m^3
Extrudates' porosity	0.59
Powder density	2.64×10^{3} kg/m^3
Powder/extrudate vol.	0.24
Bed porosity	0.36
Bed length	0.47 m
Bed 3	
Porous particles	Alumina extrudates
Mean dia. of extrudates	1.4×10^{-3} m
Nonporous particles	Silicate powder
Mean dia. of powder	0.35×10^{-3}m
Extrudates' true density	3.32×10^{3} kg/m^3
Extrudates' porosity	0.59
Powder density	2.64×10^{3} kg/m^3
Powder/extrudate vol.	0.24
Bed porosity	0.31
Bed length	0.47 m

Theoretical Studies

Cylindrical model

The problem has been studied for cylindrical particles of finite and infinite length. It is assumed that catalyst pores are completely filled with liquid (Colombo et al., 1976; Goto et al., 1981; Yentekakis and Vayenas, 1987) and that the tracer molecules can penetrate all the accessible pores of the catalyst structure. Furthermore, the catalyst particles are assumed isothermal with a uniform surface activity. External mass-transfer limitations are considered negligible, a justified assumption in oil hydrotreatment processes.

Cylinder of Finite Length. We consider four wetting configurations that are symmetric with respect to the cylinder axis, as shown in Figure 1. The effectively wetted parts of the particle external surface are:

(a_1) One base and a fraction F of the side surface.

(a_2) The two bases and a fraction F of the side surface in two zones, $F1$ and $F2$ in contact with the bases.

(a_3) A continuous fraction F of the side surface.

(a_4) A fraction F of the side surface separated in two zones $F1$ and $F2$.

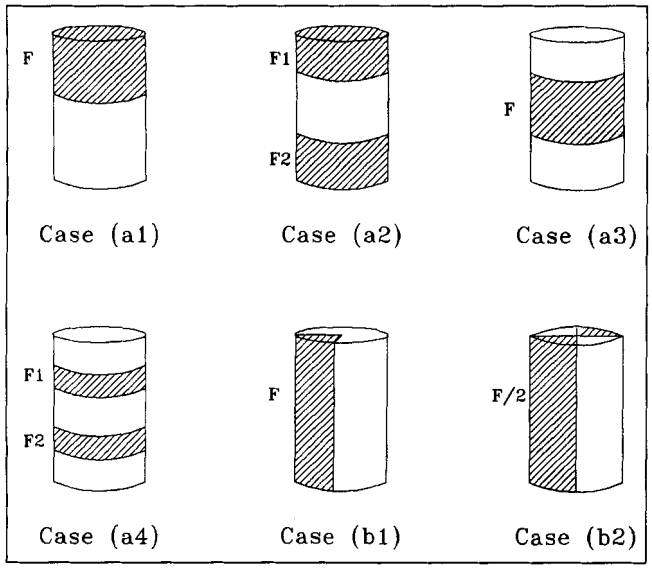

Figure 1. Wetting cases studied with the cylindrical model.

The reactant mass balance in a porous particle is described by the following second-order partial differential equation (PDE).

$$\frac{\partial^2 C}{\partial r^2} + \frac{1}{r}\cdot\frac{\partial C}{\partial r} + \frac{\partial^2 C}{\partial z_1^2} = \frac{r_0}{D_e}. \tag{1}$$

The reaction rate is expressed by a power-law-type equation:

$$r_0 = k_v \cdot C^n. \tag{2}$$

To convert Eq. 1 to dimensionless form, the following variables are used:

$$L_p = \frac{V_p}{S_p} = \frac{R}{2\cdot(1+(R/L_0))} \qquad x_1 = \frac{r}{L_p}$$

$$y_1 = \frac{z_1}{L_p} \qquad c_A = \frac{C}{C_b}. \tag{3}$$

The domain of x_1 and y_1 is

$$x_1 \in [0,2\cdot(1+(R/L_0))] \qquad y_1 \in [0,2\cdot(1+(L_0/R))].$$

From Eqs. 1, 2, and 3 the following PDE is derived:

$$\frac{\partial^2 c_A}{\partial x_1^2} + \frac{1}{x_1}\cdot\frac{\partial c_A}{\partial x_1} + \frac{\partial^2 c_A}{\partial y_1^2} = \frac{2}{n+1}\cdot\phi^2\cdot c_A^n. \tag{4}$$

The surface boundary conditions (BC) applied to solve Eq. 4 are:

For wetted base or side surface: $c_A = 1$. (5)

For nonwetted base: $\dfrac{dc_A}{dy_1} = 0.$ (6)

For nonwetted side surface: $\dfrac{dc_A}{dx_1} = 0.$ (7)

The symmetry about the cylinder axis also gives:

$$\frac{dc_A}{dx_1} = 0 \quad \text{at} \quad x_1 = 0. \tag{8}$$

For the wetting cases considered in this work, partial wetting, F_w, is given as a function of F, R, and L_0 by the Eqs. 9–12.

Case (a_1):

$$F_w = \frac{F + (R/(2\cdot L_0))}{1+(R/L_0)}. \tag{9}$$

Case (a_2):

$$F_w = \frac{F_1 + F_2 + (R/L_0)}{1+(R/L_0)}. \tag{10}$$

Case (a_3):

$$F_w = \frac{F}{1+(R/L_0)}. \tag{11}$$

Case (a_4):

$$F_w = \frac{F_1 + F_2}{1+(R/L_0)}. \tag{12}$$

The finite-difference method was employed to solve the partial differential equation, Eq. 4, along with the boundary conditions Eqs. 5–8 for a first- and second-order reaction. The resulting system was solved using the Gauss–Seidel method. The Newton linearization was followed in the case of a second-order reaction where the equations of the system were nonlinear.

The effectiveness factor n_{eff} was calculated by the following relation:

$$n_{\text{eff}} = \frac{\int_{V_p} k_v \cdot C^n \cdot dV_p}{\pi\cdot R^2\cdot L_0\cdot k_v\cdot C_b^n} = \frac{\int_{V_p} c_A^n \cdot dV_p}{\pi\cdot R^2\cdot L_0}. \tag{13}$$

The integral of Eq. 13 was calculated using the generalized Simpson rule.

Cylinder of Infinite Length. In this case two partial wetting configurations were examined as shown in Figure 1:

(b_1) An F_w fraction of the side surface is wetted. The section of this surface with a plane perpendicular to the cylinder axis gives a continuous arc of $F_w/2/\pi$ rad.

(b_2) The wetted side surface extends to two quarters, one opposite to the other.

The equation expressing the tracer mass balance in dimensionless form is

$$\frac{\partial^2 c_A}{\partial x_2^2} + \frac{1}{x_2 \cdot \pi^2} \cdot \frac{\partial c_A}{\partial x_2} \cdot \frac{\partial^2 c_A}{\partial y_2^2} = \frac{2}{n+1} \cdot \phi^2 \cdot c_A^n, \quad (14)$$

where

$$x_2 = \frac{2 \cdot r}{R}, \qquad y_2 = \frac{\varphi}{\pi}. \quad (15)$$

The domain of the independent variables is

$$x_2 \in [0,2], \qquad y_2 \in [0,2].$$

The numerical solution of PDE 14 with BC 5 and 7, which correspond to a cylinder of infinite length, is similar to that for the cylinder with finite length.

Contacting effectiveness in a trickle-bed reactor

This model includes two independent mass balances, one for the liquid flowing in the interparticle space and one for the liquid diffusing into the porous particles. The tracer concentration in the interparticle space is obtained as a function of time and axial coordinate by the following PDE:

$$D_z \cdot h_l \cdot \epsilon_{\kappa\lambda} \cdot \frac{\partial^2 c}{\partial l^2} - u_i \cdot h_l \cdot \epsilon_{\kappa\lambda} \cdot \frac{\partial c}{\partial l} - h_l \cdot \epsilon_{\kappa\lambda} \cdot \frac{\partial c}{\partial t} + \int_{A_i} N_A \, dA = 0, \quad (16)$$

where A_i denotes the external surface of the particles per unit bed volume and N_A the tracer flux through A_i. The last term of the preceding equation can be written as

$$\int_{A_i} N_A \, dA = - D_e \cdot \frac{\partial c_i}{\partial r}_{r=R} \cdot \frac{F_s}{R} \cdot (1 - \epsilon_{\kappa\lambda}).$$

Also using the correlations

$$t_d = \frac{t \cdot u_i}{L_0}, \qquad z_2 = \frac{1}{L_0}, \qquad Pe = \frac{u_i \cdot L_0}{D_z} \quad \text{and} \quad x_3 = \frac{r}{R},$$

Equation 16 is transformed to

$$\frac{1}{Pe} \cdot \frac{\partial^2 c}{\partial z_2^2} - \frac{\partial c}{\partial z_2} - \frac{\partial c}{\partial t_d} - A \cdot \frac{D_e \cdot L_0}{R^2 \cdot u_i} \cdot \frac{\partial c_i}{\partial x_3}_{x_3 = 1} = 0, \quad (17)$$

where the constant A depends on the bed porosity, $\epsilon_{\kappa\lambda}$, the external liquid holdup, h_l, and the shape of the particles, and is given by the relation:

$$A = \frac{F_s \cdot (1 - \epsilon_{\kappa\lambda})}{h_l \cdot \epsilon_{\kappa\lambda}}. \quad (18)$$

The value of the constant F_s is equal to 2 for cylinders of high L_0/R ratio and to 3 for spherical particles.

The plug-flow model is used for the sake of comparison, and it can be derived from Eq. 17, when the first term is put equal to zero ($Pe \gg 1$).

The tracer diffusion in the porous particles is described by Eq. 19, which includes two independent parameters, the effective pore wetting, h_f, and an effective diffusion coefficient, D_e:

$$\frac{\partial^2 c_i}{\partial x_3^2} + \frac{F_{s1}}{x_3} \cdot \frac{\partial c_i}{\partial x_3} - \frac{R^2 \cdot u_i \cdot h_f \cdot \epsilon_p}{D_e \cdot L_0} \cdot \frac{\partial c_i}{\partial t_d} = 0, \quad (19)$$

where the value of constant F_{s1} depends on the particle shape and is equal to 1 for cylinders of high L_0/R ratio and to 2 for spherical particles. It is assumed that the tracer is not adsorbed on the solid internal surface. This assumption was verified for the particles of porous alumina used in our experiments. It is also assumed that mass-transfer limitations in the liquid surrounding the particles are negligible. For partially wetted particles, D_e is substituted for the effective diffusion coefficient in the presence of partial wetting, D_{epw}, in Eqs. 16, 17, and 19.

The boundary and initial conditions applied to solve the system of Eqs. 17 and 19 are

$$c_i(x_3, z_2, t_d) = 0 \quad \text{for} \quad t_d = 0, \quad 0 < z_2 \le 1, \quad 0 \le x_3 < 1 \quad (20)$$

$$c(z_2, t_d) = 0 \quad \text{for} \quad t_d = 0, \quad 0 < z_2 \le 1 \quad (21)$$

$$c_i(1, z_2, t_d) = c(z_2, t_d) \quad \text{for} \quad 0 < z_2 \le 1 \quad (22)$$

$$\frac{\partial c_i(0, z_2, t_d)}{\partial x_3} = 0 \quad \text{for} \quad 0 \le z_2 \le 1, \quad t_d \ge 0 \quad (23)$$

$$c(0, t_d) - \frac{1}{Pe} \cdot \frac{\partial c(0, t_d)}{\partial z_2} = 1 \quad \text{for} \quad t_d \ge 0 \quad (24)$$

$$c(1, t_d) = 0 \quad \text{for} \quad t_d \ge 0. \quad (25)$$

As described by Eq. 17, the concentration of the tracer in the intraparticle space is a function of the position along the particle radius, of the position along the reactor axis, and of the time. In the interparticle space, the concentration of the tracer is a function of the position along the reactor axis and of the time. The problem can be considered as a second-order PDE with three independent variables, which is subject to a boundary condition in the form of a second-order PDE with two independent variables.

The system of the two PDEs cannot be solved analytically. It can be solved in the Laplace transform domain (Colombo et al., 1976). The function $c(z_2, t_d)$ and explicit expressions can be obtained from the moments of response curves. However, the use of this method is expected to introduce considerable errors because of the long tail of the responses. It must be noted that the moments of higher than first order are very sensitive to the time selected for cutting off the response curve (Sicardi et al., 1980). In this study, the solution to the problems of these systems was attempted by numerical methods.

Table 2. Region of Parameters for the Partial Wetting Cases

Case	ϕ	n	L_0/R	F
(a_1)	0.5–10	1,2	1,2,4,6,8	0.1–1
(a_2)	0.5–10	1,2	1,2,4,8	0.2–1
(a_3)	0.5–10	1	4,8	0.2–1
(a_4)	0.5–10	1	4.8	0.2–1
(b_1)	0.5–10	1		0.4–1
(b_2)	0.5–10	1		0.5

In the case of a numerical solution, two properties should be studied:

1. The convergence of the solution obtained.
2. If (1) is valid, then the approach to the real solution.

The methods selected to solve the differential equations are the finite-difference method (FDM) and the finite-element method (FEM). These methods present different characteristics in the process of building the numerical algorithm. For the FDM, implicit differences were adopted. For the FEM, bilinear functions were used as approximations of the position-independent variables and implicit differences for the time variable. The results obtained from the two methods are compared. The convergence was first examined and then the exactness of the solutions was studied.

Results and Discussion

Cylindrical model

For the partial wetting configurations selected, the impact of the following parameters on the effectiveness factor was studied:

(i) Thiele modulus, ϕ.

(ii) Reaction order, n.

(iii) Length-to-diameter ratio of the particle, L_0/R.

(iv) Effectively wetted fraction of the side surface of the cylinder, F.

The range of the values of parameters (i)–(iv) used in this study for the wetting configurations (a_1)–(a_4) and (b_1)–(b_2) is given in Table 2.

The effectiveness factor is a function of the Thiele modulus, ϕ, and partial wetting, F_w, $n_{\text{eff}} = f1(\phi, F_w)$. When $F_w = 1$, n_{eff} can be predicted from the relation n_{eff} vs. ϕ for a particle completely covered by the liquid. The Thiele modulus is proportional to the equivalent particle length $L_p = V_p/S_p$. In the case of incomplete coverage of the external surface, the external surface effectively covered by liquid, S_{ppw}, is equal to $F_w \cdot S_p$, and the active equivalent length, L_{ppw}, is equal to L_p/F_w. Thus, in the case of partial wetting, a modified Thiele modulus, ϕ_{pw} can be defined:

$$\phi_{pw} = \frac{\phi}{F_w}. \tag{26}$$

From Eq. 26, an increase of the modified Thiele modulus is observed for $F_w < 1$. An approach of the particle effectiveness factor under partial wetting conditions can be given by the relation n_{eff} vs. the Thiele modulus for complete wetting if ϕ_{pw} substitutes for ϕ. Typical cases of the errors involved by using this modification are presented in Figures 2–5. The different points representing the values of n_{eff} calculated by the solution of the corresponding model are compared with the approximate solution given by the solid line. From Figures 2–5 it is observed that the use of the modified Thiele modulus results in a good approximation of n_{eff}. The devia-

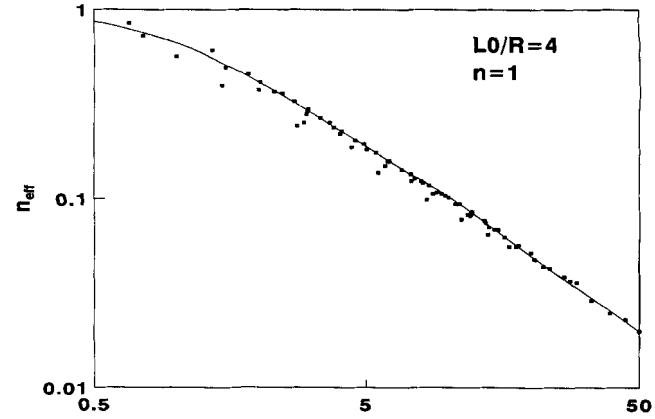

Figure 3. Calculated n_{eff} by the model (■) vs. approximate n_{eff} (—).
Case (a_1). $F_w = 0.18$–0.82.

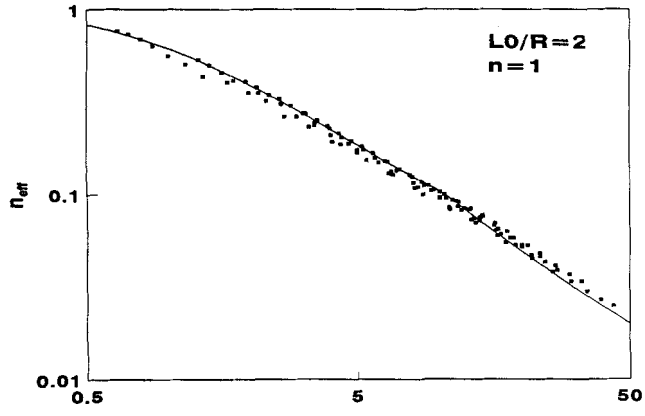

Figure 2. Calculated n_{eff} by the model (■) vs. approximate n_{eff} (—).
Case (a_1). $F_w = 0.23$–0.77.

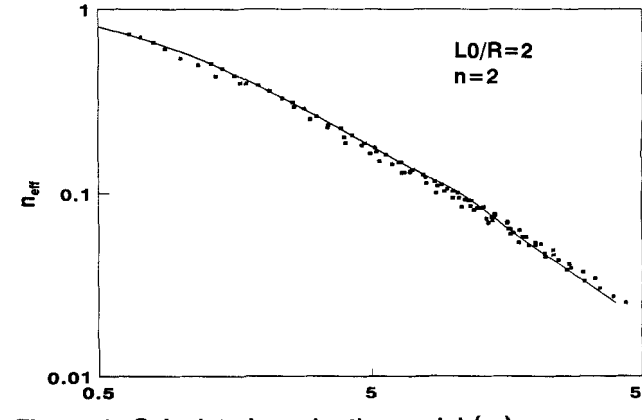

Figure 4. Calculated n_{eff} by the model (■) vs. approximate n_{eff} (—).
Case (a_1). $F_w = 0.23$–0.77.

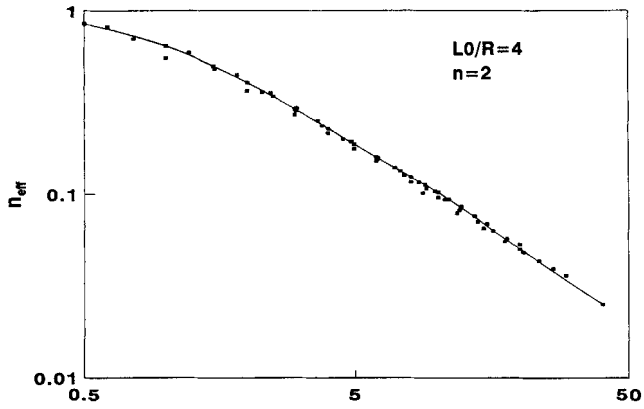

Figure 5. Calculated n_{eff} by the model (■) vs. approximate n_{eff} (—).

Case (a_1). $F_w = 0.34$–0.82.

tions between the effectiveness factor values calculated from the numerical solution, n_{eff}, and determined by using the modified Thiele modulus, n_{eff_full}, are examined on the basis of the mean relative error given by the formula:

$$\text{ERR\_FT} = \frac{\sum_{i=1}^{N_i} \left(1 - \frac{n_{eff}[i]}{n_{eff\_full}[i]}\right)^2}{N_j}, \qquad (27)$$

where N_j is the number of the discrete values of ϕ used for a particular type and degree of partial wetting.

In Figure 6, ERR_FT values are presented as a function of the partial wetting degree, F_w. As observed, ERR_FT tends to decrease as the degree of partial wetting increases. For partial-wetting degrees greater than 0.6, which is of practical interest (Satterfield, 1975; Colombo et al., 1976), the error level is lower than 0.1. For all the cases examined, ERR_FT takes the following mean values, MV_ERR_FT, and standard deviation values, SD_ERR_FT:

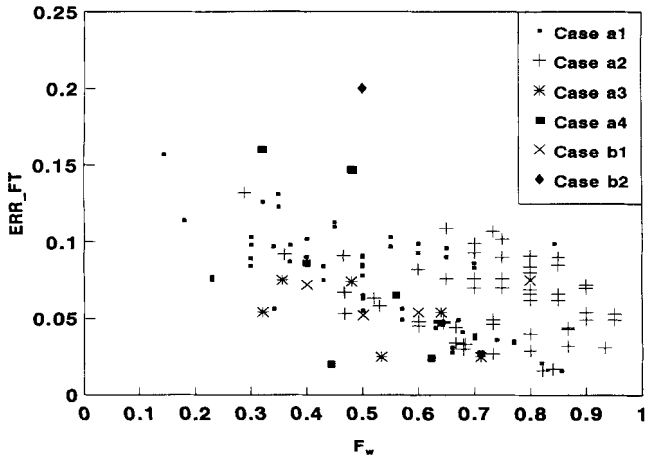

Figure 6. Mean relative error, ERR_FT, as a function of partial wetting, F_w.

MV_ERR_FT = 0.0917,

SD_ERR_FT = 0.0378 for $F_w < 0.6$ $n = 1$

MV_ERR_FT = 0.0548,

SD_ERR_FT = 0.0244 for $F_w \geq 0.6$ n = 1

MV_ERR_FT = 0.0841,

SD_ERR_*FT* = 0.0217 for $F_w < 0.6$ n = 2

M*V*_ERR_FT = 0.0593,

SD_ERR_FT = 0.0258 for $F_w \geq 0.6$ n = 2.

These results indicate that n_{eff} for partially wetted cylindrical particles can be approximated by the correlations of effectiveness factor vs. the Thiele modulus for totally wetted particles by using the modified Thiele modulus given by Eq. 26. From this equation, a practical estimate of F_w can be extracted:

$$\phi_{pw} = \frac{V_p}{S_p \cdot F_w} \cdot \sqrt{\frac{(n+1) \cdot k_v \cdot C_b^{n-1}}{2 \cdot D_e}} = \frac{V_p}{S_p} \cdot \sqrt{\frac{(n+1) \cdot k_v \cdot C_b^{n-1}}{2 \cdot D_e \cdot F_w^2}} = \frac{V_p}{S_p} \cdot \sqrt{\frac{(n+1) \cdot k_v \cdot C_b^{n-1}}{2 \cdot D_{epw}}}. \qquad (28)$$

We can see that if we do not take the degree of partial wetting into account reduced effective diffusion coefficients will result from the treatment of the experimental data. The following formula for F_w is derived from Eq. 28:

$$F_w = \sqrt{\frac{D_{epw}}{D_e}}. \qquad (29)$$

As a result, F_w can be estimated from the effective diffusion coefficient under partial wetting conditions, D_{epw}, and the effective diffusion coefficient for full liquid coverage of the external surface of the catalyst, D_e.

The cases of partial wetting we have examined can be characterized as geometrical. Under real process conditions the external wetting of the particles should be a combination of the preceding cases. From Figure 6 it can be seen that for a given partial-wetting degree the manner of wetting does not practically influence the values of ERR_FT. On the other hand, the values of MV_ERR_FT are found in the range of the error of experimentation. This means that Eq. 29 can be safely used for the evaluation of the partial-wetting degree.

Contacting effectiveness in the trickle-bed reactor

Theoretical Examination of the Numerical Methods. Here we study the convergence of the developed algorithms and the approximation of the exact solution by the numerical solutions. The three parameters that influence the numerical solutions are:

Table 3. Bed Characteristics and Process Conditions

	Bed a	Bed b	Bed c
Particle shape	Spherical	Cylindrical	Cylindrical diluted with nonporous powder of 0.35×10^{-3} m, dia.
Particle dia., m	0.35×10^{-3}	1.4×10^{-3}	1.4×10^{-3}
Particle porosity	0.59	0.59	0.59
Bed porosity	0.44	0.46	0.31
Bed length, m	0.46	0.474	0.46
Bed cross section, m^2	4.3×10^{-4}	4.3×10^{-4}	4.3×10^{-4}
Temp., °C	350	350	350
Pres., bar	50	50	50
Liquid feed flow rate, kg/s	4.17×10^{-5}	1.39×10^{-5} 2.22×10^{-5} 4.17×10^{-5} 8.33×10^{-5}	2.22×10^{-5} 4.17×10^{-5}
Gas feed flow rate, Nm^3/s	1.1×10^{-5}	1.1×10^{-5}	1.1×10^{-5}

(i) Constant of partitioning of the dimensionless particle radius, M.

(ii) Constant of partitioning of the dimensionless reactor length, N.

(iii) Time step of integration, dt.

A trickle bed of porous Al_2O_3 in powder form was simulated. The bed characteristics, bed (a), and the process conditions are given in Table 3. For the effective diffusion coefficient, a value of 1×10^{-11} m^2/s was used.

The values of M, N, and dt selected for the FEM and FDM are given in Tables 4 and 5. The representative response curves for the FEM are shown in Figure 7. In all cases, the solution converges, but it appears to be sensitive to the values of N. Estimation of an approximation of the solutions obtained for the exact solution cannot be made from these results. For second-order finite-difference methods, except partitioning values, the solution is influenced by the value of the constant $k = dt_d/dx^2$, where dx is the position differential. The algorithm does not converge for k values greater than a high limit. This implies that the use of high values of M and N imposes a decrease on the dt_d value so that a convergent solution can be obtained.

Table 4. Domain Partitioning for FEM

Symbols	M	N	dt
20,30,3	20	30	180
20,40,3	20	40	180
20,60,3	20	60	180
20,60,6	20	60	360
20,80,6	20	80	360
20,100,6	20	100	360
10,80,3	10	80	180
25,80,3	25	80	180

Table 5. Domain Partitioning for FDM

Symbols	M	N	dt
20,30,3	20	30	180
20,40,3	20	40	180
20,60,6	10	60	360
20,80,6	20	80	360

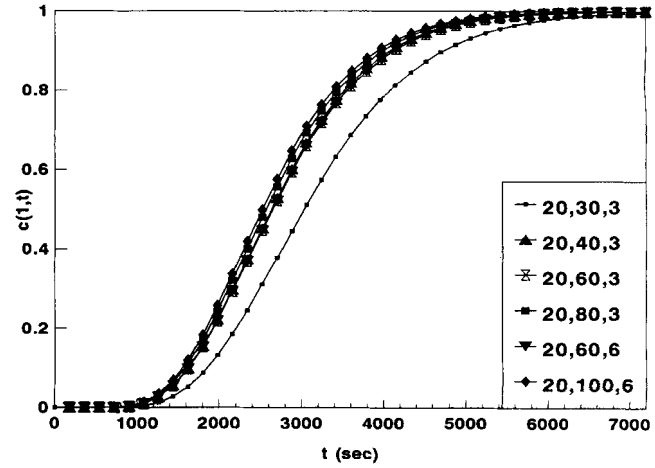

Figure 7. Response curves for *M,N,dt* sets using FEM.

In Figure 8, response curves for the FDM are shown. The solutions obtained do not vary significantly in comparison with the ones obtained with FEM. Convergence of the solutions obtained by the two methods (FDM and FEM) to the exact solution can be accepted if there are sets of values of M,N, and dt for which the solutions for the FEM and FDM are the same. It is assumed that the solution for the FDM and $(M, N, dt) = (20, 40, 3)$ represents the exact solution because the values of dt_d/dz_2^2 and dt_d/dx_3^2 are very low. The deviations of the tracer concentration at the bed outlet between the calculated values obtained with the 20,40,3 set and other sets of M,N,dt (deviation $= c_{M,N,dt} - c_{20,40,3}$) for the FDM are presented in Figure 9. A maximum deviation of 1% appears for the set (20,30,3). In Figure 10, the deviations obtained between the solutions for the FEM and the exact solution are shown. It is obvious that the two methods tend to give the same solution, and as a consequence this solution should be a good approximation of the exact one. For both methods a partitioning of $M = 20$ is proved to be satisfactory. Even so, FEM needs $N = 80$–100 to approximate the exact solution, while FDM needs only $N = 40$. This makes FDM more efficient in comparison with FEM, which uses bilinear functions as approximates and needs more computation time than FDM.

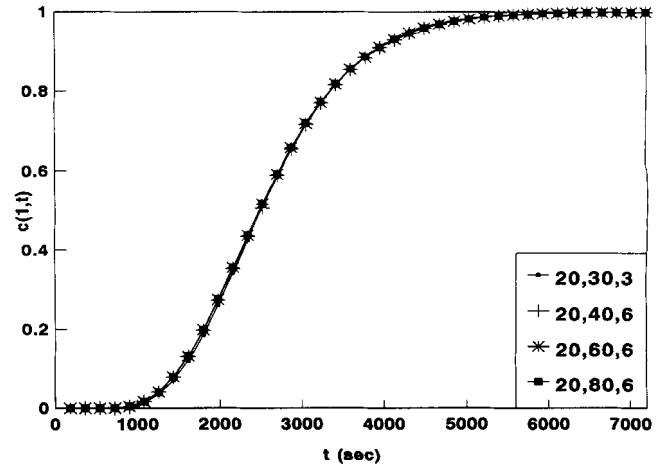

Figure 8. Response curves for *M,N,dt* sets using FDM.

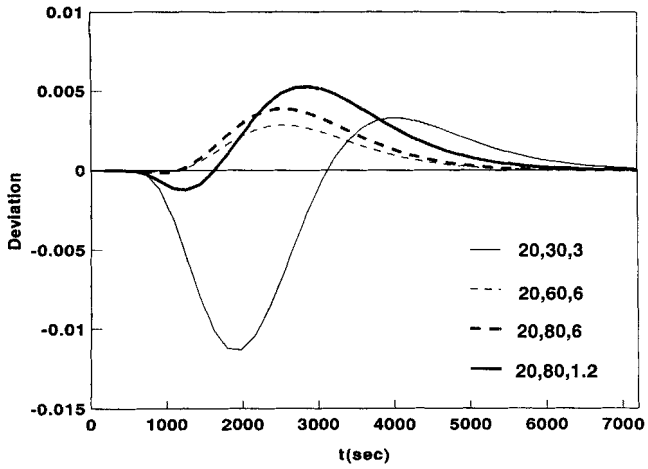

Figure 9. Deviations in the output concentration between *M,N,dt* sets and 20, 40, 3 of FDM.

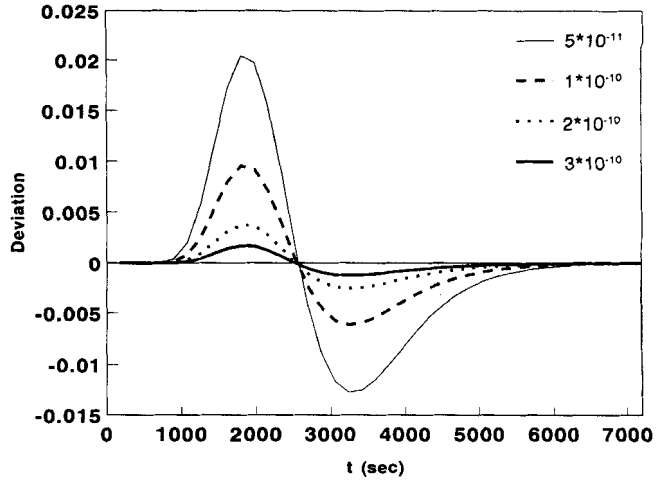

Figure 11. Differences between output concentrations for various D_e and $D_e = 5\times10^{-10}$: bed (a).

Experimental Design. The experiments were designed so that significant differences in the expected values of effective diffusion coefficients would produce significantly different response curves. The particle sizes were defined on this basis for the flow rates used in conventional experiments.

The simulation was based on data from previous experimentation in our laboratory (Tsamatsoulis, 1993), and it was applied to a bed of porous powder with a mean diameter of 0.35×10^{-3} m. In Table 3, the characteristics of the bed are presented. The liquid flowrate was chosen 4.17×10^{-5} kg/s. The response curves were calculated for $D_e = 5\times10^{-11}$, 1×10^{-10}, 2×10^{-10}, 3×10^{-10}, and 5×10^{-10} m^2/s. In order to examine the influence of D_e values on the response curves, the differences between the tracer output concentration for a given D_e and for $D_e = 5\times10^{-10}$ m^2/s, $C_{D_e} - C_{5\cdot10^{-10}}$, were calculated and are shown in Figure 11. We can see that the differences cannot be considered significant. An order of magnitude reduction of the D_e values, from 5×10^{-10} to 5×10^{-11} m^2/s, causes a maximum difference of 2% between the response curves. This implies that larger particles must be used for the experimental evaluation of the effective diffusion coefficients.

Two beds, (b) and (c), were considered, and their characteristics and the process conditions are given in Table 3. The differences $c_{D_e} - c_{5\cdot10^{-10}}$ calculated for bed (b) and $Q = 8.33\times10^{-5}$ kg/s are presented in Figure 12. The deviations obtained in this case are measurable. The percentage of maximum differences between the concentration values derived for $D_e = 1\times10^{-10}$, 2×10^{-10}, 3×10^{-10} m^2/s and those obtained for $D_e = 5\times10^{-10}$ m^2/s are presented in Table 6 for the beds (b) and (c).

The results presented in Figures 11 and 12 and in Table 6 indicate that the model can be applied to beds packed with extrudates of 1.4×10^{-5} m in diameter or greater, undiluted or diluted with nonporous powder. The usual commercial hydrotreatment catalysts have diameters within this range.

Application of the Model to Real Process Conditions. The proposed model was used to analyze the residence time distribution (RTD) curves obtained from the three beds whose characteristics were given in Table 1. The values of the axial dispersion coefficient and holdup were calculated from data

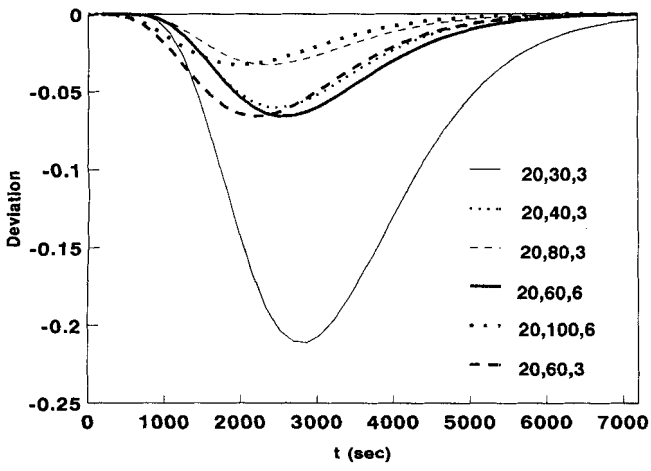

Figure 10. Deviations in the output concentration between *M,N,dt* sets of FEM and 20, 40, 3 for FDM.

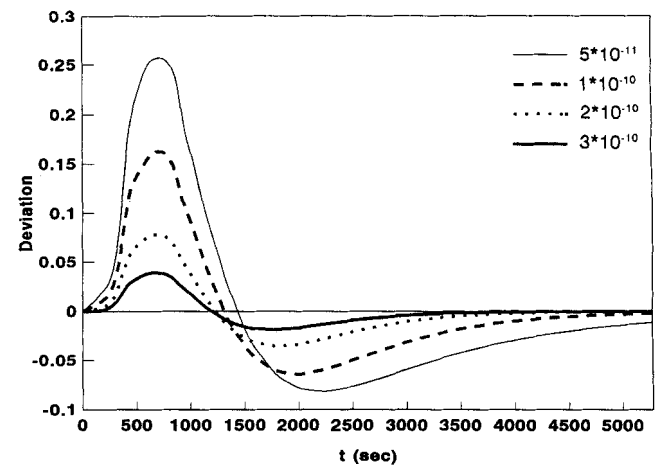

Figure 12. Differences between output concentrations for various D_e and $D_e = 5\times10^{-10}$: bed (b).

Table 6. Maximum % Difference Between Response Curves for $D_e = 5\times10^{-10}$ and $D_e = 1\times10^{-10}$–3×10^{-10} m²/s

Q (kg/s)	D_e (m²/s) 1×10^{-10}	2×10^{-10}	3×10^{-10}
	Bed b		
1.39×10^{-5}	6	2.6	1.2
2.22×10^{-5}	8	3.4	1.7
4.17×10^{-5}	12	5.4	2.6
8.33×10^{-5}	16	7.8	3.9
	Bed c		
2.22×10^{-5}	7	3	1.4
4.17×10^{-5}	9.8	4.3	2

presented in a recent work (Tsamatsoulis and Papayannakos, 1994). For the sake of comparison, the plug-flow model was also applied. Using a nonlinear regression technique, the effective diffusion coefficient, D_e, and internal partial wetting, h_f, were calculated. In Table 7, the mean values of D_e and h_f are presented as a function of the actual liquid velocity u_i, for the axial dispersion model and the plug flow.

It is obvious that the effective diffusion coefficient values calculated using the plug-flow model, $D_{e\,plug}$, are much lower than those computed by the axial dispersion model, $D_{e\,ax.disp}$. For the three beds studied, the mean value of the ratio $D_{e\,plug}/D_{e\,ax.disp}$ is equal to 0.30. A small decrease appears in the h_f values estimated using the plug flow. In this case, the mean value of $h_{f\,plug}/h_{f\,ax.disp}$ is equal to 0.92. These results indicate that the application of the plug-flow model leads to a severe underestimation of D_e values. As a consequence, this model cannot be used with much confidence in trickle-bed laboratory reactors for the estimation of internal mass transfer phenomena in porous catalysts.

As discussed previously, partial wetting can be expressed by Eq. 31. The maximum value of the effective diffusion coefficient, D_{eMAX}, is assumed to represent the effective diffusion coefficient that corresponds to full external wetting. Figure 13 shows the dependence of $\sqrt{D_e/D_{eMAX}}$ on the actual liquid velocity. It is observed that for the diluted beds and for

Table 7. Mean Values of Effective Diffusion Coefficient, D_e, and Pore Filling h_f

$u_i\times10^4$ m/s	$D_e\times10^{10}$ m²/s Axial Disp.	Plug Flow	h_f Axial Disp.	Plug Flow
		Bed 1		
5.3	2.1	0.50	0.83	0.75
6.88	1.8	0.68	0.89	0.86
8.53	1.7	0.58	0.78	0.75
10.53	3.2	0.86	0.80	0.74
		Bed 2		
2.2	1.5	0.57	0.72	0.68
3.27	2.6	0.76	0.84	0.73
3.98	3.9	1.3	0.82	0.70
5.17	4.3	1.2	0.79	0.71
6.42	4.7	1.7	0.85	0.76
7.97	4.3	1.2	0.83	0.73
		Bed 3		
3.87	3.1	0.96	0.86	0.76
5.42	4.6	1.5	0.97	0.89
6.73	4.5	1.3	0.94	0.93
8.10	4.9	1.3	0.96	0.87

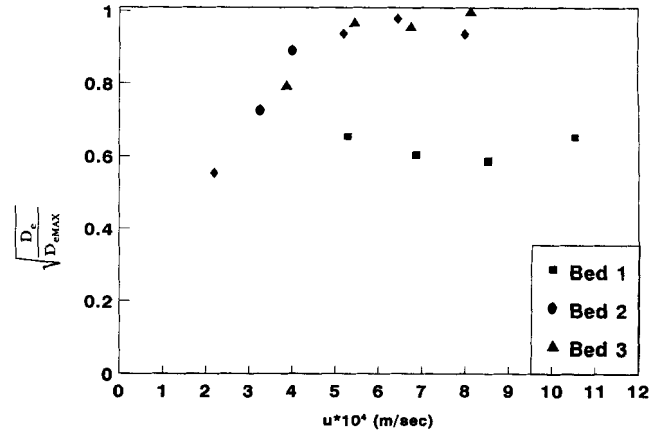

Figure 13. Dependence of $\sqrt{D_e/D_{eMAX}}$ on the liquid velocity u_i for beds 1, 2, 3.

velocity values higher than 5×10^{-4} m/s, the degree of partial wetting is greater than or equal to 0.94. In this case, external wetting can be considered as complete, taking experimental error into account. Thus, the assumption of full wetting for the flow rate where D_e takes its maximum value is considered true with a high degree of confidence. Partial external wetting is also observed in the diluted beds for velocities lower than 5×10^{-4} m/s. Low values of F_w were calculated for nondiluted bed number 1 in the range of the velocities studied. For 13 out from 14 experimental points, the degree of partial wetting is greater than 0.60, in accordance with data in the literature (Satterfield, 1975; Colombo, 1976). It is indicated that bed dilution greater or equal to 0.25 volume of diluent to volume of porous particles, $V_{dil}/V_{Al_2O_3}$, improves partial wetting of the particle's external surface area. For liquid velocities greater than $\sim 5\times10^{-4}$ m/s, external effective wetting is expected to approach 1. An observed improvement in the bed performance following dilution with fine inert particles is mentioned by several investigators (van Klinken and van Dongen, 1980; de Bruijn, 1976; Carruthers and diCamillo, 1988). The liquid velocities needed for full wetting nondiluted beds are high, as shown in Figure 13, and beyond the space velocity range used in small reactors.

The amount of the pore volume penetrated by the tracer molecules was determined in this study using an experimental tracer method and subsequent analysis. The dependence of internal wetting, h_f, on the liquid velocity is shown in Figure 14. Internal wetting appears to be independent of the liquid velocity, with a mean value equal to 0.85 and standard deviation equal to 0.07. A combination of the degree of partial internal wetting and the particle pore volume distribution can indicate the portion of the particle pore volume that is accessible to the tracer. Figure 15 shows the frequency of the pore volume distribution of the Al_2O_3 particles used. A bimodal pore radius distribution is observed with a maximum in the region of 1,500 Å (mesoporosity) and a second maximum in the region of 30 Å (microporosity). Thus, pores with radii in the microporosity range are barely penetrated by the sulfur compounds of the oil used in RTD experimentation, which was a typical HVGO. According to the pore distribution, the value of $h_f = 0.85$ implies an intrusion of the tracer molecules into pores with radius greater than 29 Å. In the

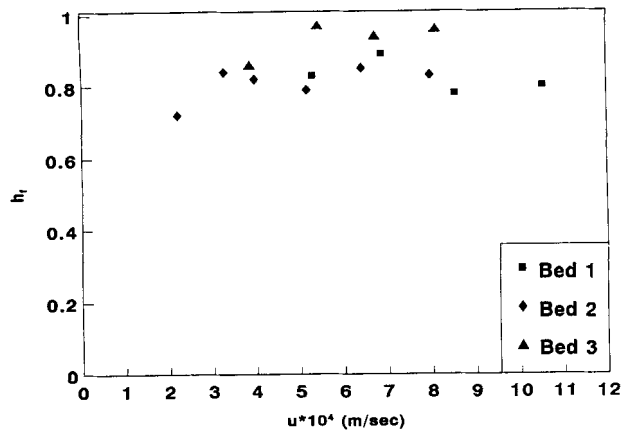

Figure 14. Dependence of actual pore filling, h_f, on the liquid velocity u_i for beds 1, 2, 3.

case of hydrodesulfurization of heavy petroleum fractions, the fine pores of the support, $r < 30$ Å, don't seem to contribute to the process because they are not accessible to the reactant molecules. However, they may be filled with small hydrocarbon molecules that do not contain sulfur compounds, due to capillary forces. This conclusion is related to the technology of the preparation of catalyst supports. The degree of internal wetting cannot be considered maximum, but instead as a function of the pore size distribution of the catalyst particles and of the compounds of interest as well. Moreover, the independence of the degree of internal wetting from the liquid flow rate implies a reduction in the number of the modeling parameters in scaling-up or -down studies by allowing the use of a uniform intrinsic reaction rate constant. This constant is proportional to the internal catalyst surface accessible to the reactants, in systems like the one under consideration.

Conclusions

The following conclusions can be drawn from the two models developed.

1. External partial wetting can be accounted for in engineering calculations by using a modified Thiele modulus.

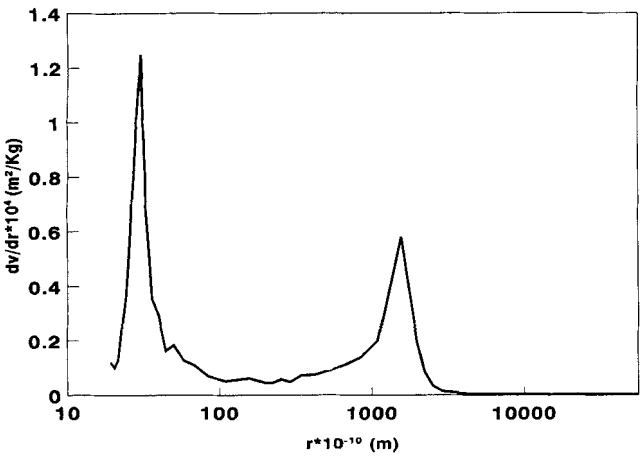

Figure 15. Frequency of the pore volume distribution of the alumina particles.

2. At partial wetting conditions, the effectiveness factor n_{eff} can be approximated by the relation n_{eff} vs. ϕ, where the modified Thiele modulus, ϕ_{pw}, must be used instead of ϕ. In the vast majority of cases studied, the error of estimation of the effectiveness factor was less than 10%, which is in the range of experimental error.

3. The external partial wetting degree, F_w, can be estimated from the effective diffusion coefficient for partial wetting conditions, D_{epw} and the corresponding one for full wetting, D_e.

4. The manner in which particles are externally wetted does not have a significant impact on the value of the effectiveness factor for a given partial wetting degree. Partial wetting at operating conditions can be considered as a compromise of the nondynamic geometrical cases examined.

5. The two numerical methods applied as an estimation of the contacting effectiveness in trickle-bed reactors give convergent solutions and approach the exact solution, but with different partitioning in the area of the independent variables.

6. The finite-difference method (FDM) proved to be more efficient than the finite-element method (FEM) with bilinear functions as approximates, because it needs significantly less computation time.

7. The contacting effectiveness model can be applied to beds of catalyst extrudates of 1.4×10^{-3} m or greater in diameter, undiluted or diluted with nonporous particles.

8. The particles of the undiluted bed of porous alumina of 1.4×10^{-3} m diameter are externally partially wetted over the whole range of the liquid velocities studied.

9. For the beds of Al_2O_3 extrudates 1.4×10^{-3} m diameter diluted with nonporous silica sand 0.35×10^{-3} m in diameter and in proportions $V_{dil}/V_{Al_2O_3} > 0.25$, the values of external partial particle wetting are higher than those of undiluted beds.

10. In diluted beds F_w increases as actual velocity u_i increases. For $u_i > 5\times10^{-4}$ m/s, external wetting is practically complete.

11. Internal wetting is incomplete and constant in all cases, $h_f = 0.85$, due to the existence of fine pores with $r < 30$ Å. Fine pores of catalysts appear to be inaccessible to sulfur compounds in hydrodesulfurization processes of heavy petroleum fractions.

Notation

C = reactant concentration in the pores of the particle in Eq. 1, kg/m^3
c = dimensionless tracer concentration in the interparticle space in Eqs. 16 and 17
c_A = reactant concentration
C_b = reactant concentration in the interparticle space, kg/m^3
c_i = tracer concentration in the intraparticle space in Eqs. 17 and 19
dt_d = dimensionless time step
dz_2 = dimensionless differential axial length
D_z = axial dispersion coefficient, m^2/s
k_v = specific reaction rate, kg^{1-n}/s/m^{3n}
l = axial reactor coordinate in Eq. 16
L_0 = cylinder length in Eqs. 3 and 9–12; reactor length in Eqs. 17 and 19, m
Pe = Peclet number
Q = liquid mass flow rate, kg/s
q = liquid volumetric flow rate, m^3/s
r = radial coordinate in Eq. 1, m

R = cylinder radius, m
S_0 = reactor cross section, m^2
S_p = external particle surface area, m^2
t = time, s
t_d = dimensionless time
$u_i = q/(S_0 \cdot \epsilon_{\kappa\lambda} \cdot h_l)$
V_p = particle volume, m^3
x_1 = dimensionless radial coordinate of the cylindrical carriers in Eq. 4
x_2 = dimensionless radial coordinate of the cylindrical carriers in Eq. 14
x_3 = dimensionless radial coordinate of the cylindrical carriers in Eqs. 17 and 19
y_1 = dimensionless cylinder axial coordinate in Eq. 4
y_2 = dimensionless angular coordinate in Eq. 14
z_1 = axial coordinate of the cylindrical carriers in Eq. 1, m
z_2 = dimensionless axial reactor coordinate in Eqs. 17 and 19
ϵ_p = particle porosity
φ = angle coordinate, rad

Literature Cited

de Bruijn, A., "Testing of HDS Catalysts in Small Trickle Phase Reactors," paper B34, Int. Cong. on Catalysis, London (1976).

Carruthers, J. D., and D. J. diCamillo, "Pilot Plant Testing of Hydrotreating Catalysts: Influence of Catalyst Condition, Bed Loading and Dilution," *Appl. Cat.*, **43**, 253 (1988).

Colombo, A. J., G. Baldi, and S. Sicardi, "Solid-liquid Contacting Effectiveness in Trickle Bed Reactors," *Chem. Eng. Sci.*, **31**, 1101 (1976).

Duducovic, M. P., "Catalyst Effectiveness Factor and Contacting Efficiency in Trickle-Bed Reactors," *AIChE J.*, **23**, 940 (1977).

Duducovic, M. P., and P. L. Mills, "Catalyst Effectiveness Factor in Trickle Bed Reactor," *Int. Symp. Chem. React. Eng.*, Adv. in Chemistry Ser., **65**, 387 (1978).

Gianetto, A., G. Baldi, V. Specchia, and S. Sicardi, "Hydrodynamics and Solid-Liquid Contacting Effectiveness in Trickle-bed Reactors," *AIChE J.*, **24**, 1087 (1978).

Goto, S., A. Lakota, and J. Levec, "Effectiveness Factor of nth Order Kinetics in Trickle-bed Reactors," *Chem. Eng. Sci.*, **36**, 157 (1981).

Herskowitz, M., "Wetting Efficiency in Trickle-bed Reactors. The Overall Effectiveness Factor of Partially Wetted Catalyst Particles," *Chem. Eng. Sci.*, **36**, 1665 (1981).

Mears, D. E., "The Role of Liquid Holdup and Effective Wetting in the Performance of Trickle Bed Reactors," *Chem. React. Eng. II*, Advances in Chemistry Ser., **133**, 218 (1974).

Mills, P. L., and M. P. Duducovic, "Analysis of Catalyst Effectiveness in Trickle Bed Reactors Processing Volatile or Nonvolatile Reactants," *Chem. Eng. Sci.*, **35**, 2267 (1980).

Mills, P. L., and M. P. Duducovic, "Evaluation of Liquid-Solid Contacting in Trickle Bed Reactors by Tracer Methods," *AIChE J.*, **28**, 893 (1981).

Morita, S., and J. M. Smith, "Mass Transfer and Contacting Efficiency in a Trickle Bed Reactor," *Ind. Eng. Chem. Fundam.*, **17**, 113 (1978).

Parascos, J. A., and J. A. Frayer, "Effect of Holdup Incomplete Catalyst Wetting and Backmixing during Hydroprocessing in Trickle Bed Reactors," *Ind. Eng. Chem. Process Des. Dev.*, **14**, 315 (1975).

Ramachandran, P. A., and J. M. Smith, "Effectiveness Factors in Trickle Bed Reactors," *AIChE J.*, **25**, 538 (1979).

Satterfield, C. N., "Trickle Bed Reactors," *AIChE J.*, **21**, 209 (1975).

Schwartz, J. G., E. Weger, and M. P. Duducovic, "A New Tracer Method for Determination of Liquid–Solid Contacting Efficiency in Trickle Bed Reactors," *AIChE J.*, **22**, 894 (1976).

Schiesser, W. E., and L. Lapidus, "Further Studies of Fluid Flow and Mass Transfer in Trickle Beds," *AIChE J.*, **28**, 163 (1961).

Sicardi, S., G. Baldi, and V. Specchia, "Hydrodynamic Models for the Interpretation of the Liquid Flow in Trickle Bed Reactors," *Chem. Eng. Sci.*, **35**, 1775 (1980).

Tan, C. S., and J. M. Smith, "Catalyst Particle Effectiveness with Unsymmetrical Boundary Conditions," *Chem. Eng. Sci.*, **35**, 1601 (1980).

Tsamatsoulis, D., "Simulation of the Operation of the Catalytic Trickle Bed Reactors," PhD Thesis, National Technical Univ. of Athens (1993).

Tsamatsoulis, D., and N. Papayannakos, "Axial Dispersion and Holdup in a Bench-scale Trickle-bed Reactor at Operating Conditions," *Chem. Eng. Sci.*, **49**, 523 (1994).

van Gelder, K. B., and K. R. Westerterp, "Residence Time Distribution and Holdup in a Concurrent Upflow Packed Bed Reactor at Elevated Pressure," *Chem. Eng. Technol.*, **13**, 27 (1990).

van Klinken, J., and R. H. van Dongen, "Catalyst Dilution for Improved Performance of Laboratory Trickle-bed Reactors," *Chem. Eng. Sci.*, **35**, 59 (1980).

Yentekakis, I. V., and C. G. Vayenas, "Effectiveness Factors for Reactions between Volatile and Non-volatile Components in Partially Wetted Catalysts," *Chem. Eng. Sci.*, **42**, 1323 (1987).

Manuscript received Jan. 10, 1995, and revision received Nov. 13, 1995.